Eur. Phys. J. A **31**, 207–212 (2007)
DOI 10.1140/epja/i2006-10172-y

THE EUROPEAN PHYSICAL JOURNAL A

Regular Article – Hadron Physics

Leading-order $2\pi\gamma$ exchange NN interaction: Central potentials proportional to g_A^0 and g_A^2

N. Kaiser[a]

Physik Department T39, Technische Universität München, D-85747 Garching, Germany

Received: 10 November 2006 / Revised: 22 December 2006
Published online: 25 January 2007 – © Società Italiana di Fisica / Springer-Verlag 2007
Communicated by U.-G. Meißner

Abstract. We calculate at two-loop order in chiral perturbation theory the electromagnetic corrections to the leading-order 2π exchange NN interaction proportional to g_A^0 and g_A^2. The resulting $2\pi\gamma$ exchange potential contains isospin-breaking components which reach up to about -2% of the corresponding isovector 2π exchange potential. With a value of only $-17\,\mathrm{keV}$ at $r = m_\pi^{-1} = 1.4\,\mathrm{fm}$ the charge-independence breaking central potential obtained here is negligibly small in comparison to the one generated by the isoscalar c_3 contact vertex. Our calculation confirms that the largest long-range isospin-violating NN potentials arise from the $2\pi\gamma$ exchange diagrams involving the large low-energy constants $c_4 \simeq -c_3 \simeq 3.3\,\mathrm{GeV}^{-1}$ representing the important $\Delta(1232)$ dynamics.

PACS. 12.20.Ds Specific calculations – 13.40.Ks Electromagnetic corrections to strong- and weak-interaction processes – 21.30.Cb Nuclear forces in vacuum

1 Introduction and summary

Isospin-violation in the nuclear force is a subject of current interest. Significant advances in the understanding of nuclear isospin-violation have been made in the past years by employing methods of effective field theory (in particular chiral perturbation theory). Van Kolck *et al.* [1] were the first to calculate (in a manifestly gauge-invariant way) the complete leading-order pion-photon exchange nucleon-nucleon interaction. In addition, the charge-independence and charge-symmetry breaking effects arising from the pion mass difference $m_{\pi^+} - m_{\pi^0} = 4.59\,\mathrm{MeV}$ and the nucleon mass difference $M_n - M_p = 1.29\,\mathrm{MeV}$ on the (leading order) two-pion exchange NN potential have been worked out in refs. [2,3]. Epelbaum and Meißner [4] have continued this line of approach by deriving the subleading isospin-breaking 2π exchange NN potentials and classifying the relevant isospin-breaking four-nucleon contact terms. Some next–to–leading-order corrections to the $\pi\gamma$ exchange potential (*i.e.* those proportional to the large isovector magnetic moment $\kappa_v = 4.7$) as well as effects from virtual $\Delta(1232)$-isobar excitation on the $\pi\gamma$ exchange interaction have been calculated in ref. [5]. All these long-range (pion-induced) isospin-breaking NN potentials have turned out to be rather weak. Typically, their values at a nucleon distance of $r = m_\pi^{-1} = 1.4\,\mathrm{fm}$ lie below $50\,\mathrm{keV}$ in magnitude (see herefore figs. 7 and 8 in ref. [4] and tables I and II in ref. [5]).

In a recent work [6] we have calculated the electromagnetic (*i.e.* one-photon exchange) corrections to the dominant two-pion exchange NN interaction. The latter comes in form of a strongly attractive isoscalar central potential and it is generated by a one-loop triangle diagram involving the isoscalar $\pi\pi NN$ contact vertex proportional to the large low-energy constant $c_3 \simeq -3.3\,\mathrm{GeV}$ [7]. The dynamics behind this large value of c_3 is (mainly) the excitation of the low-lying $\Delta(1232)$-resonance. It has been found that this particular class of two-loop $2\pi\gamma$ exchange diagrams (proportional to c_3) leads to sizable charge-independence and charge-symmetry breaking central potentials which amount to $0.3\,\mathrm{MeV}$ at $r = m_\pi^{-1}$ [6]. The effect of the other equally strong low-energy constant $c_4 \simeq 3.4\,\mathrm{GeV}$ [7] entering in an isovector spin-flip $\pi\pi NN$ contact vertex has also been studied. Somewhat weaker charge-independence breaking spin-spin and tensor potentials with values of $-0.11\,\mathrm{MeV}$ and $0.09\,\mathrm{MeV}$ at $r = m_\pi^{-1}$ have been found. Although they arise from contact vertices at next-to-leading order in the small momentum expansion these $2\pi\gamma$ exchange potentials (proportional to c_3 and c_4) are the largest long-range isospin-violating NN potentials obtained so far. For a further confirmation of this remarkable finding one should also evaluate and quantify the isospin-violating $2\pi\gamma$ exchange interaction at leading order in the chiral expansion. This is the purpose of the present pa-

[a] e-mail: nkaiser@ph.tum.de

per. We will restrict ourselves here to the classes of two-loop diagrams which scale as g_A^0 and g_A^2 with the nucleon axial vector coupling constant $g_A = g_{\pi N} f_\pi / M_N \simeq 1.3$ (choosing the recent value $g_{\pi N} = 13.15$ [8] of the pion-nucleon coupling constant). The pertinent spectral functions (or imaginary parts) are calculated analytically for each contributing diagram and these expressions are then used to compute the NN potential in coordinate space. As a largest isospin-violating component we find a charge-independence breaking central potential ($\sim \tau_1^3 \tau_2^3$) of size $-17\,\mathrm{keV}$ at $r = m_\pi^{-1}$. Our results therefore confirm that the $2\pi\gamma$ exchange interaction follows closely the pattern observed for the chiral 2π exchange NN interaction in refs. [7,9]. The next–to–leading-order contributions dominate over the leading-order ones due to the presence of the large low-energy constants $c_4 \simeq -c_3 \simeq 3.3\,\mathrm{GeV}^{-1}$ representing the important $\Delta(1232)$ dynamics.

Our paper is organized as follows. In sect. 2 we present first analytical expressions for the spectral functions of the two-loop $2\pi\gamma$ exchange diagrams proportional to g_A^0 and g_A^2. These results are then used in sect. 3 to evaluate numerically the corresponding central NN potentials in coordinate space which include the isospin-violating components of interest. We present also a rough estimate for the (remaining) class of diagrams proportional to g_A^4.

2 Two-loop spectral functions

We are interested in the long-range part of the coordinate space potential generated by certain two-loop $2\pi\gamma$ exchange diagrams. For that purpose it is sufficient to know the spectral functions or imaginary parts of these two-loop diagrams. Making use of (perturbative) unitarity in the form of the Cutkosky cutting rule we can calculate the two-loop spectral functions as integrals of the (subthreshold) $\bar{N}N \to \pi\pi\gamma \to \bar{N}N$ transition amplitudes over the Lorentz-invariant $2\pi\gamma$ three-particle phase space. In the (conveniently chosen) center-of-mass frame this leads to two angular integrations and two integrals over the (on-shell) pion energies. Due to the heavy nucleon limit ($M_N \to \infty$) and the masslessness of the photon ($m_\gamma = 0$) several simplifications occur and therefore most of these integrations can actually be performed in closed analytical form. For a concise presentation of our results it is furthermore advantageous to scale out all common (dimensionful) parameters from the spectral function

$$\mathrm{Im}\, T(i\mu) = \frac{\alpha\, m_\pi^2}{\pi^2 (4 f_\pi)^4}\, S\left(\frac{\mu}{m_\pi}\right), \tag{1}$$

and to work with the dimensionless variable $u = \mu/m_\pi$ where, $\mu \geq 2m_\pi$ denotes the $\pi\pi\gamma$ invariant mass. Here, $\alpha = 1/137.036$ is the electromagnetic fine-structure constant, $m_\pi = 139.57\,\mathrm{MeV}$ denotes the (charged) pion mass and $f_\pi = 92.4\,\mathrm{MeV}$ stands for the weak pion decay constant.

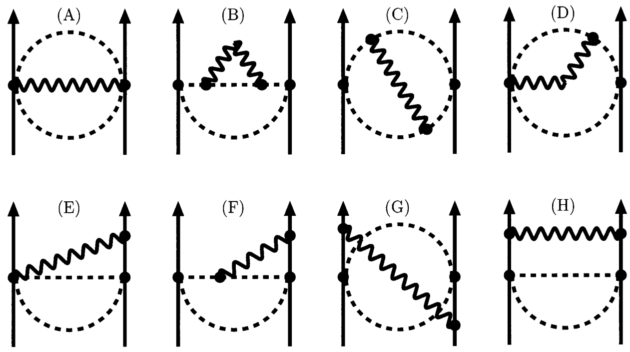

Fig. 1. Electromagnetic corrections to the 2π exchange bubble diagram proportional to g_A^0. Diagrams turned upside-down and diagrams with the role of both nucleons interchanged are not shown. The spectral function $\mathrm{Im}\, T(i\mu)$ is calculated by cutting the intermediate $\pi\pi\gamma$ three-particle state.

2.1 Diagrams proportional to g_A^0

We add to the 2π exchange bubble diagram (scaling as g_A^0) a photon line which runs from one side to the other. There are five positions for the photon to start at the left-hand side and five positions to arrive at the right-hand side. These 25 diagrams (each with a combinatoric factor of 1/2) are obtained from the eight representative ones shown in fig. 1 by adding horizontally and/or vertically reflected partners[1]. We are working throughout in the Feynman gauge, where the photon propagator is proportional to $g_{\mu\nu}$. The Feynman rules for the various effective chiral vertices can be found in appendix A of ref. [10]. Without going into further technical details, related to isospin factors and solving elementary integrals, we enumerate now the contributions of the eight representative diagrams (A)–(H) shown in fig. 1 to the dimensionless spectral $S(u)$. We find for $u \geq 2$:

$$S(u)^{(\mathrm{A})} = (\vec{\tau}_1 \cdot \vec{\tau}_2 + 3\tau_1^3 \tau_2^3)\left\{ -\frac{u^2+2}{8u}\sqrt{u^2-4} + \left(1 - \frac{1}{u^2}\right) \ln \frac{u + \sqrt{u^2-4}}{2} \right\}, \tag{2}$$

where $\vec{\tau}_{1,2}$ are the usual isospin operators with third components $\tau_{1,2}^3$.

$$S(u)^{(\mathrm{B})} = (\vec{\tau}_1 \cdot \vec{\tau}_2 + \tau_1^3 \tau_2^3)\left\{ \frac{2-6u^2+5u^4-u^6}{3u^4} \ln \frac{u+\sqrt{u^2-4}}{2} + \frac{6-u^2+u^4}{36u^3}\sqrt{u^2-4} + \frac{4}{3u}(u^2-4) \oint_1^{u/2} \mathrm{d}x\, \frac{y}{u-2x} \right\}, \tag{3}$$

[1] Diagram (F) still has to be duplicated by another one, where the photon emanates from the lower pion line.

with the abbreviation $y = \sqrt{x^2-1}$.

$$S(u)^{(\mathrm{C})} = \tau_1^3\tau_2^3 \left\{ \frac{68u^2-12-23u^4}{36u^3}\sqrt{u^2-4} + \frac{5u^6-26u^4+34u^2-4}{3u^4} \times \ln\frac{u+\sqrt{u^2-4}}{2} + \frac{2}{3u^2}(6u^2-8-u^4) \times \oint_1^{u/2} \frac{\mathrm{d}x}{u-2x}\ln\frac{u(x+y)-1}{u(x-y)-1}\right\}, \tag{4}$$

$$S(u)^{(\mathrm{D})} = (\vec\tau_1\cdot\vec\tau_2 + 3\tau_1^3\tau_2^3)\left\{\frac{3}{16u}(u^2-2)\sqrt{u^2-4} + \left(1-\frac{u^2}{4}-\frac{3}{2u^2}\right)\ln\frac{u+\sqrt{u^2-4}}{2}\right\}. \tag{5}$$

The contribution of diagram (E) vanishes, $S(u)^{(\mathrm{E})} = 0$, because the isospin factor is equal to zero.

$$S(u)^{(\mathrm{F})} = (\vec\tau_1\cdot\vec\tau_2 - \tau_1^3\tau_2^3)\left\{\frac{53u^4+874u^2-8}{144u^3}\sqrt{u^2-4} + \frac{21u^6-296u^4-234u^2-8}{36u^4}\ln\frac{u+\sqrt{u^2-4}}{2} + \oint_1^{u/2}\frac{\mathrm{d}x}{u-2x}\left[\frac{8y}{9u}(u^2-28) + \left(8-\frac{2u^2}{3}\right)\ln\frac{u-x+y}{u-x-y}\right]\right\}, \tag{6}$$

$$S(u)^{(\mathrm{G+H})} = (\vec\tau_1\cdot\vec\tau_2 - \tau_1^3\tau_2^3)\left\{\left(\frac{1}{u^2}-\frac{1}{3}\right)\ln\frac{u+\sqrt{u^2-4}}{2} + \frac{50-11u^2}{72u}\sqrt{u^2-4} + \frac{4}{3u}(u^2-4)\oint_1^{u/2}\mathrm{d}x\,\frac{y}{u-2x}\right\}. \tag{7}$$

The contribution from diagram (G) together with the irreducible part of diagram (H) is proportional to the difference of their isospin factors on the left nucleon line, $[1+\tau_1^3, \tau_1^c]\epsilon^{abc} = 2i(\tau_1^a\delta^{b3} - \tau_1^b\delta^{a3})$. The "encircled" integrals appearing in eqs. (3), (4), (6), (7) symbolize the following regularization prescription:

$$\oint_1^{u/2}\mathrm{d}x\,\frac{f(x)}{u-2x} = \int_1^{u/2}\mathrm{d}x\,\frac{f(x)-f(u/2)}{u-2x}. \tag{8}$$

This regularization prescription eliminates from some contributions to the spectral function $S(u)$ an infrared singularity due to the emission of soft photons ($\bar NN \to \pi\pi\gamma_{\mathrm{soft}}$). The singular factor $(u-2x)^{-1}$ stems (mostly) from a pion propagator. The regularization prescription defined in eq. (8) is equivalent to the familiar "plus"-prescription employed commonly for parton splitting functions in order to eliminate there an analogous infrared singularity due to soft-gluon radiation [11]. It has also been used in our previous works [6]. It would, of course, by desirable to extend the present calculational framework such that the overall infrared finiteness could be demonstrated in detail. It is then conceivable that additional contributions beyond the "plus"-regularization prescription emerge which might quantitatively modify the numerical results for the isospin-violating NN potentials. We note as an aside that the non-elementary integrals ($\int_1^{u/2}\mathrm{d}x\ldots$) in eqs. (4), (6) could be solved in terms of dilogarithms, whereas

$$\oint_1^{u/2}\mathrm{d}x\,\frac{4\sqrt{x^2-1}}{u-2x} = \sqrt{u^2-4}\ln\frac{u+2}{e} - u\ln\frac{u+\sqrt{u^2-4}}{2}, \tag{9}$$

is still expressible in terms of elementary functions. Finally, it is interesting to observe that no charge-symmetry breaking terms $\sim \tau_1^3+\tau_2^3$ are generated by the $2\pi\gamma$ exchange diagrams in fig. 1.

2.2 Diagrams proportional to g_A^2

Next, we turn to the class of diagrams proportional to g_A^2. We add to the 2π exchange triangle diagram a photon line which runs from one side to the other. There are five positions for the photon to start on the left-hand side and now seven positions to arrive at the right-hand side. Leaving out those four diagrams which vanish in the Feynman gauge (with photon propagator proportional to $g_{\mu\nu}$) we get the sixteen representative diagrams shown in fig. 2. Except for diagram (I) these are to be understood as being duplicated by horizontally reflected partners. A further doubling of the number of diagrams comes from interchanging the role of both nucleons. Obviously, diagram (II) vanishes in the Feynman gauge, $S(u)^{(\mathrm{II})} = 0$, (since

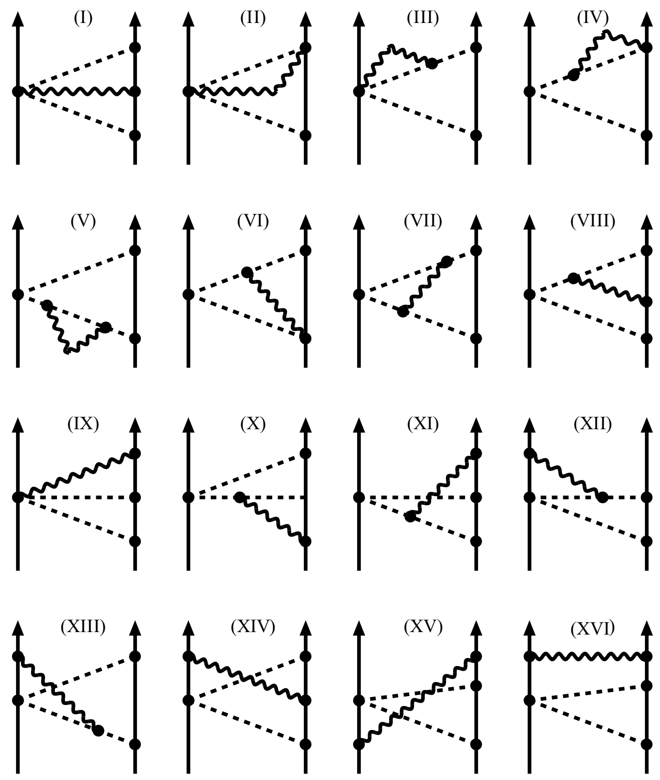

Fig. 2. Electromagnetic corrections to the 2π exchange triangle diagram proportional to g_A^2. Diagrams with the contact vertex at the right nucleon line and diagrams turned upside-down are not shown. The spectral function $\mathrm{Im}\,T(i\mu)$ is calculated by cutting the intermediate $\pi\pi\gamma$ three-particle state.

$g_{0i}=0$) and the remaining contributions to the dimensionless spectral function $S(u)$ read for $u\geq 2$:

$$S(u)^{(\mathrm{I})}=g_A^2(\vec\tau_1\cdot\vec\tau_2+\tau_1^3\tau_2^3-\tau_1^3-\tau_2^3)\bigg\{\bigg(2-\frac{2}{u^2}\bigg)\times\ln\frac{u+\sqrt{u^2-4}}{2}-\frac{u^2+2}{4u}\sqrt{u^2-4}+\iint d\omega_1\,d\omega_2(u^2+2-4u\,\omega_1)\frac{\arccos(-\hat k_1\cdot\hat k_2)}{|\vec k_1\times\vec k_2|}\bigg\}. \quad (10)$$

Here, $(\omega_1,\vec k_1)$ and $(\omega_2,\vec k_2)$ denote the four-momenta of the two on-shell pions in units of the pion mass with $|\vec k_j|=\sqrt{\omega_j^2-1}$. A circumflex on a symbol denotes the corresponding unit vector. The negative scalar product of the two pion-momenta is given by the quadratic polynomial: $-\vec k_1\cdot\vec k_2=u(\omega_1+\omega_2)-\omega_1\omega_2-1-u^2/2$. The double integral in eq. (10) extends over that region inside the square $1\leq\omega_{1,2}\leq u/2$ where the radicand in the denominator $|\vec k_1\times\vec k_2|^2=2u\,\omega_1\omega_2(\omega_1+\omega_2)-(u^2+1)(\omega_1+\omega_2)^2-u^2\omega_1\omega_2+(u^3+2u)(\omega_1+\omega_2)-u^2-u^4/4$ is positive.

$$S(u)^{(\mathrm{III})}=g_A^2(\vec\tau_1\cdot\vec\tau_2+3\tau_1^3\tau_2^3)\bigg\{\frac{11u^2-6}{16u}\sqrt{u^2-4}+\bigg(3-\frac{5u^2}{4}-\frac{3}{2u^2}\bigg)\ln\frac{u+\sqrt{u^2-4}}{2}\bigg\}, \quad (11)$$

$$S(u)^{(\mathrm{IV})}=g_A^2(\vec\tau_1\cdot\vec\tau_2+\tau_1^3\tau_2^3)\bigg\{\frac{11u^2-6}{8u}\sqrt{u^2-4}+\bigg(6-\frac{5u^2}{2}-\frac{3}{u^2}\bigg)\ln\frac{u+\sqrt{u^2-4}}{2}\bigg\}, \quad (12)$$

$$S(u)^{(\mathrm{V})}=g_A^2(\vec\tau_1\cdot\vec\tau_2+\tau_1^3\tau_2^3)\bigg\{\frac{2}{3u^4}(19u^4-5u^6-6u^2-2)\times\ln\frac{u+\sqrt{u^2-4}}{2}+\frac{17u^4-35u^2-6}{18u^3}\sqrt{u^2-4}+\frac{8}{3u}(5u^2-8)\oint_1^{u/2}dx\,\frac{y}{u-2x}\bigg\}, \quad (13)$$

$$S(u)^{(\mathrm{VI})}=g_A^2\tau_1^3\tau_2^3\bigg\{\frac{34-u^2}{4u}\sqrt{u^2-4}+\bigg(\frac{34}{u^2}+\frac{6}{u^2-1}+u^2-22\bigg)\ln\frac{u+\sqrt{u^2-4}}{2}+\frac{8}{u}\int_1^{u/2}dx\,\frac{ux-2}{y^2}\ln\frac{u(x+y)-1}{u(x-y)-1}\bigg\}, \quad (14)$$

$$S(u)^{(\mathrm{VII})}=g_A^2\tau_1^3\tau_2^3\bigg\{\frac{6-115u^2-2u^4}{9u^3}\sqrt{u^2-4}+\frac{4}{3u^4}(2+4u^2-11u^4+8u^6)\ln\frac{u+\sqrt{u^2-4}}{2}+\frac{4}{u^2}\int_1^{u/2}\frac{dx}{y^2}(6u-u^3-4x-u^2x)\times\ln\frac{u(x+y)-1}{u(x-y)-1}+\frac{4}{3u^2}(18u^2-16-5u^4)\times\oint_1^{u/2}\frac{dx}{u-2x}\ln\frac{u(x+y)-1}{u(x-y)-1}\bigg\}, \quad (15)$$

$$S(u)^{(\mathrm{VIII})}=g_A^2(\tau_1^3+\tau_2^3-\tau_1^3\tau_2^3-\vec\tau_1\cdot\vec\tau_2)\bigg\{\bigg[\frac{3}{2u^2}-\frac{3}{2}-\frac{5u^2}{4}+\frac{3}{2(u^2-1)}\bigg]\ln\frac{u+\sqrt{u^2-4}}{2}+\frac{3}{16u}(7u^2+2)\sqrt{u^2-4}+\int_1^{u/2}\frac{dx}{y^2}\times\bigg(3x-u-\frac{2}{u}\bigg)\ln\frac{u(x+y)-1}{u(x-y)-1}\bigg\}, \quad (16)$$

$$S(u)^{(\mathrm{IX})}=g_A^2(\tau_1^3+\tau_2^3+2\tau_1^3\tau_2^3)\bigg\{\bigg(2-\frac{2}{u^2}\bigg)\times\ln\frac{u+\sqrt{u^2-4}}{2}-\frac{u^2+2}{4u}\sqrt{u^2-4}+\iint d\omega_1\,d\omega_2\Big[4u(\omega_1+\omega_2)-2u^2-4\Big]\frac{\arccos(-\hat k_1\cdot\hat k_3)}{|\vec k_1\times\vec k_2|}\bigg\}, \quad (17)$$

with $\vec k_3=-\vec k_1-\vec k_2$ the photon momentum of magnitude $|\vec k_3|=u-\omega_1-\omega_2$ and the negative scalar product given by the quadratic polynomial $-\vec k_1\cdot\vec k_3=(\omega_1+\omega_2)(\omega_1-u)+u^2/2$.

$$S(u)^{(\mathrm{X})}=g_A^2(\tau_1^3+\tau_2^3+\tau_1^3\tau_2^3+\vec\tau_1\cdot\vec\tau_2)\times\bigg\{\frac{4-18u^2+238u^4+75u^6}{36u^4}\ln\frac{u+\sqrt{u^2-4}}{2}+\frac{4+4u^2-535u^4}{144u^3}\sqrt{u^2-4}+\oint_1^{u/2}\frac{dx}{u-2x}\times\bigg[\frac{4y}{9u}(17u^2-8)-\frac{5u^2}{3}\ln\frac{u-x+y}{u-x-y}\bigg]\bigg\}, \quad (18)$$

$$S(u)^{(\mathrm{XI})}=g_A^2(\tau_1^3+\tau_2^3+3\tau_1^3\tau_2^3-\vec\tau_1\cdot\vec\tau_2)\bigg\{\oint_1^{u/2}\frac{dx}{u-2x}\times\bigg[\frac{4y}{9u}(8-17u^2)+\frac{5u^2}{3}\ln\frac{u-x+y}{u-x-y}\bigg]+\frac{173u^4-29u^2-2}{72u^3}\times\sqrt{u^2-4}+\int_1^{u/2}\frac{dx}{y^2}\bigg(u-3x+\frac{2}{u}\bigg)\ln\frac{u(x+y)-1}{u(x-y)-1}-\bigg[\frac{5u^2}{6}+\frac{46}{9}+\frac{1}{u^2}+\frac{1}{9u^4}+\frac{3}{2(u^2-1)}\bigg]\ln\frac{u+\sqrt{u^2-4}}{2}\bigg\}, \quad (19)$$

$$S(u)^{(\mathrm{XII})}=g_A^2(2+\tau_1^3+\tau_2^3+\tau_1^3\tau_2^3-\vec\tau_1\cdot\vec\tau_2)\times\bigg\{-\frac{8+54u^2+152u^4+105u^6}{72u^4}\times\ln\frac{u+\sqrt{u^2-4}}{2}+\frac{611u^4-98u^2-8}{288u^3}\sqrt{u^2-4}+\oint_1^{u/2}\frac{dx}{u-2x}\bigg[\frac{4y}{9u}(8-17u^2)+\frac{5u^2}{3}\ln\frac{u-x+y}{u-x-y}\bigg]\bigg\}, \quad (20)$$

Table 1. The isovector 2π exchange central potential $\widetilde{W}_C^{(2\pi)}(r)$ proportional to g_A^0 and electromagnetic corrections to it as a function of the nucleon distance r. The values in the third row correspond to the isospin-violating central potential $\widetilde{V}_C^{(\text{cib})}(r)$.

r [fm]	0.9	1.0	1.1	1.2	1.3	1.4	1.5	1.6	1.7	1.8
$\widetilde{W}_C^{(2\pi)}$ [MeV]	0.637	0.353	0.205	0.124	0.077	0.049	0.032	0.022	0.015	0.010
$\widetilde{W}_C^{(0)}$ [keV]	−8.06	−3.89	−1.97	−1.04	−0.570	−0.320	−0.184	−0.108	−0.064	−0.038
$\widetilde{V}_C^{(\text{cib})}$ [keV]	−2.94	−1.65	−0.975	−0.596	−0.376	−0.243	−0.161	−0.108	−0.074	−0.052

Table 2. The isovector 2π exchange central potential $\widetilde{W}_C^{(2\pi)}(r)$ proportional to g_A^2 and electromagnetic corrections to it as a function of the nucleon distance r. The values in the fourth and fifth row correspond to the isospin-violating central potentials $\widetilde{V}_C^{(\text{cib})}(r)$ and $\widetilde{V}_C^{(\text{csb})}(r)$.

r [fm]	0.9	1.0	1.1	1.2	1.3	1.4	1.5	1.6	1.7	1.8
$\widetilde{W}_C^{(2\pi)}$ [MeV]	11.96	6.75	3.99	2.45	1.56	1.01	0.677	0.460	0.319	0.224
$\widetilde{V}_C^{(0)}$ [keV]	25.44	14.19	8.30	5.04	3.16	2.04	1.34	0.903	0.618	0.429
$\widetilde{W}_C^{(0)}$ [keV]	−49.70	−20.34	−8.33	−3.24	−1.07	−0.156	0.201	0.313	0.322	0.290
$\widetilde{V}_C^{(\text{cib})}$ [keV]	−232.9	−127.4	−73.1	−43.6	−26.9	−17.1	−11.1	−7.38	−4.99	−3.43
$\widetilde{V}_C^{(\text{csb})}$ [keV]	−25.44	−14.19	−8.30	−5.04	−3.16	−2.04	−1.34	−0.903	−0.618	−0.429

$$
\begin{aligned}
S(u)^{(\text{XIII})} &= g_A^2(2+\tau_1^3+\tau_2^3-\tau_1^3\tau_2^3+\vec{\tau}_1\cdot\vec{\tau}_2)\\
&\times\bigg\{\frac{8+54u^2+152u^4+105u^6}{72u^4}\ln\frac{u+\sqrt{u^2-4}}{2}\\
&+\frac{8+98u^2-611u^4}{288u^3}\sqrt{u^2-4}+\oint_1^{u/2}\frac{\mathrm{d}x}{u-2x}\\
&\times\left[\frac{4y}{9u}(17u^2-8)-\frac{5u^2}{3}\ln\frac{u-x+y}{u-x-y}\right]\bigg\}, \qquad (21)
\end{aligned}
$$

$$
S(u)^{(\text{XIV})} = g_A^2(\vec{\tau}_1\cdot\vec{\tau}_2-1)\,\frac{\pi^2}{3u}(u^3-6u+4), \qquad (22)
$$

$$
\begin{aligned}
S(u)^{(\text{XV+XVI})} &= g_A^2(\tau_1^3\tau_2^3-\vec{\tau}_1\cdot\vec{\tau}_2)\bigg\{\left(\frac{2}{u^2}-\frac{50}{3}\right)\\
&\times\ln\frac{u+\sqrt{u^2-4}}{2}+\frac{50+133u^2}{36u}\sqrt{u^2-4}\\
&+\frac{8}{3u}(8-5u^2)\oint_1^{u/2}\mathrm{d}x\,\frac{y}{u-2x}\\
&+\iint \mathrm{d}\omega_1\mathrm{d}\omega_2\Big[4u(\omega_1+\omega_2)-2u^2-4\Big]\frac{\arccos(-\hat{k}_1\cdot\hat{k}_3)}{|\vec{k}_1\times\vec{k}_2|}\bigg\}. \qquad (23)
\end{aligned}
$$

The "encircled" integrals appearing in eqs. (13), (15), (18)–(21), (23) involve again the regularization prescription defined in eq. (8). We have also checked gauge invariance. The (total) spectral function $S(u)$ stays ξ-independent when adding a longitudinal part to the photon propagator: $g_{\mu\nu}\to g_{\mu\nu}+\xi k_\mu k_\nu$.

3 $2\pi\gamma$ exchange potential in coordinate space

Now we are in the position to present numerical results. For orientation let us first recall the isovector central potential ($\sim \vec{\tau}_1\cdot\vec{\tau}_2$) generated by the leading-order 2π exchange bubble and triangle diagrams. As a function of the nucleon distance r, it reads [9]

$$
\begin{aligned}
\widetilde{W}_C^{(2\pi)}(r) &= \frac{2\pi m_\pi}{(4\pi f_\pi r)^4}\Big\{[1+2g_A^2(5+2z^2)]K_1(2z)\\
&+z(1+10g_A^2)K_0(2z)\Big\}, \qquad (24)
\end{aligned}
$$

with $z=m_\pi r$ and $K_{0,1}(2z)$ two modified Bessel functions. The numerical values in the first rows of tables 1 and 2 display the magnitude and r-dependence of this weakly repulsive 2π exchange potential separated into its contributions proportional to g_A^0 and g_A^2. One observes that the g_A^2-component is more than a factor of 20 larger than the other one. This feature comes from the different combinatoric factors and the different large-r asymptotics of the contributions from the bubble and triangle diagram.

With the help of the spectral function $\mathrm{Im}\,T(i\mu)$ or $S(u)$ the $2\pi\gamma$ exchange central potential in coordinate space $\widetilde{V}_C^{(2\pi\gamma)}(r)$ can be easily calculated via a modified Laplace transformation:

$$
\begin{aligned}
\widetilde{V}_C^{(2\pi\gamma)}(r) &= -\frac{1}{2\pi^2 r}\int_{2m_\pi}^\infty \mathrm{d}\mu\,\mu e^{-\mu r}\,\mathrm{Im}\,T(i\mu)\\
&= \widetilde{V}_C^{(0)}(r)+\vec{\tau}_1\cdot\vec{\tau}_2\,\widetilde{W}_C^{(0)}(r)\\
&+\tau_1^3\tau_2^3\,\widetilde{V}_C^{(\text{cib})}(r)+(\tau_1^3+\tau_2^3)\,\widetilde{V}_C^{(\text{csb})}(r), \qquad (25)
\end{aligned}
$$

where we have given in the second and third lines of eq. (25) the decomposition into isospin-conserving (0), charge-independence breaking (cib) and charge-symmetry breaking (csb) parts. The numbers in the second and third row of table 1 and the second to fifth row of table 2 display the dropping of the $2\pi\gamma$ exchange central potentials $V_C^{(0)}(r)$, $\widetilde{W}_C^{(0)}(r)$, $\widetilde{V}_C^{(\text{cib})}(r)$ and $\widetilde{V}_C^{(\text{csb})}(r)$ with the nucleon distance r in the region $0.9\,\mathrm{fm} \le r \le 1.8\,\mathrm{fm}$. When focusing on the isospin-violating components one observes a strong suppression of the contribution from the class of diagrams scaling as g_A^0, similar to the original 2π exchange potential $\widetilde{W}_C^{(2\pi)}(r)$. As the largest isospin-violating component one identifies the charge-independence breaking potential coming from the class of diagrams proportional to g_A^2, with a value of $-17\,\mathrm{keV}$ at $r = m_\pi^{-1} = 1.4\,\mathrm{fm}$. This is almost a factor of 20 smaller than the one generated by the isoscalar $\pi\pi NN$ contact vertex proportional to $c_3 = -3.3\,\mathrm{GeV}^{-1}$ which had a strength of 303 keV [6] at $r = m_\pi^{-1}$. It is also instructive to compare the isospin-violating $2\pi\gamma$ exchange potentials with the isospin-conserving 2π exchange potential. Their maximal relative ratio of about 1.7% is consistent with the usual rule of thumb estimate, namely, $\alpha/\pi \simeq 1/430$ times a numerical factor. In the present case this numerical factor is not just 1 but of the order 7, due to the large number of contributing diagrams. From that point of view the relative smallness of the leading-order $2\pi\gamma$ exchange potential is not surprising. The electromagnetic (one-photon exchange) corrections follow closely the pattern observed for the chiral 2π exchange NN potential [9,7]. The next–to–leading-order contributions dominate considerably over the leading-order ones due to presence of the large low-energy constants $c_4 \simeq -c_3 \simeq 3.3\,\mathrm{GeV}^{-1}$ [7] representing the important $\Delta(1232)$ dynamics.

At leading order there is also the class of $2\pi\gamma$ exchange diagrams scaling as g_A^4 with the axial vector coupling constant $g_A = g_{\pi N} f_\pi / M_N \simeq 1.3$. For some (out of these $7 \cdot 7 \cdot 2 = 98$) diagrams with four nucleon propagators the presently used method to calculate the spectral functions as a three-body phase-space integral does not properly work anymore in the heavy nucleon limit $M_N \to \infty$. The reason for this failure is that in some cases the two-loop spectral function (in the limit $M_N \to \infty$) starts (discontinuously) with a non-vanishing value at the threshold $\mu = 2m_\pi$. As discussed in the appendix of ref. [12] a μ-dependent spectral function with such a behavior cannot be represented by a regular three-body phase-space integral. In view of the expected calculational complexity we restrict ourselves here to a crude estimate of the isospin-violating parts $\sim g_A^4$. The leading-order isovector central potential $\widetilde{W}_C^{(2\pi)}(r)$ proportional to g_A^4 has a value of $-4.40\,\mathrm{MeV}$ at $r = 1.4\,\mathrm{fm}$ (see herefore eq. (42) in ref. [9]). Allowing for a relative size of the electromagnetic correction of -1.5%[2] one estimates the possible isospin-violating component to about 66 keV. This is still small compared to the 303 keV [6] from the isoscalar c_3 contact vertex. Moreover, the leading-order isoscalar spin-spin and tensor potentials $\widetilde{V}_{S,T}^{(2\pi)}(r)$ proportional to g_A^4 have values of 2.30 MeV and $-2.23\,\mathrm{MeV}$ at $r = 1.4\,\mathrm{fm}$ (see eqs. (44), (41) in ref. [9]). With the above rule of estimation this gives isospin-violating spin-spin and tensor potentials of magnitude 35 keV, again small compared to the effects from the c_4 contact vertex obtained in ref. [6].

Altogether, our explicit calculation of the leading-order $2\pi\gamma$ exchange diagrams proportional to g_A^0 and g_A^2 together with the rule of thumb estimate of the g_A^4-contributions confirms that the largest long-range isospin-violating NN potentials are the ones generated by the $c_{3,4}$ contact vertices representing the important $\Delta(1232)$ dynamics. In order to test their phenomenological relevance these should be included into future NN phase shift analyses and few-body calculations.

References

1. U. van Kolck, M.C.M. Rentmeester, J.L. Friar, T. Goldman, J.J.de Swart, Phys. Rev. Lett. **80**, 4386 (1998).
2. J.L. Friar, U. van Kolck, Phys. Rev. C **60**, 034006 (1999).
3. J.L. Friar, U. van Kolck, G.L. Payne, S.A. Coon, Phys. Rev. C **68**, 024003 (2003).
4. E. Epelbaum, Ulf-G. Meißner, Phys. Rev. C **72**, 044001 (2005).
5. N. Kaiser, Phys. Rev. C **73**, 044001 (2006).
6. N. Kaiser, Phys. Rev. C **73**, 064006 (2006); **74**, 067001 (2006).
7. E. Epelbaum, Prog. Part. Nucl. Phys. **57**, 654 (2006) and references therein.
8. R.A. Arndt, W.J. Briscoe, I.I. Strakovsky, R.L. Workman, Phys. Rev. C **74**, 045205 (2006).
9. N. Kaiser, R. Brockmann, W. Weise, Nucl. Phys. A **625**, 758 (1998).
10. V. Bernard, N. Kaiser, Ulf-G. Meißner, Int. J. Mod. Phys. E **4**, 193 (1995).
11. M.E. Peskin, D.V. Schroeder, *Quantum Field Theory* (Addison-Wesley Publishing Company, 1995) Chapt. 17.5.
12. N. Kaiser, Phys. Rev. C **62**, 024001 (2000).

[2] In the case of the dominant c_3-terms [6] the relative size of the electromagnetic correction has been -1.2%.